

High Time-Resolved Imaging of Targets in Turbid Media Using Ultrafast Optical Kerr Gate

This content has been downloaded from IOPscience. Please scroll down to see the full text.

2012 Chinese Phys. Lett. 29 024207

(<http://iopscience.iop.org/0256-307X/29/2/024207>)

View [the table of contents for this issue](#), or go to the [journal homepage](#) for more

Download details:

IP Address: 117.32.153.157

This content was downloaded on 26/03/2014 at 10:02

Please note that [terms and conditions apply](#).

High Time-Resolved Imaging of Targets in Turbid Media Using Ultrafast Optical Kerr Gate *

TONG Jun-Yi(佟俊仪), TAN Wen-Jiang(谭文疆), SI Jin-Hai(司金海)**, CHEN Feng(陈烽),
YI Wen-Hui(易文辉), HOU Xun(侯洵)

Key Laboratory for Physical Electronics and Devices of the Ministry of Education, Shaanxi Key Lab of Information Photonic Technique, School of Electronics and Information Engineering, Xi'an Jiaotong University, Xi'an 710049

(Received 11 November 2011)

We demonstrate the ultrafast imaging of a submillimeter bar chart that is either hidden behind glass diffusers or inside a solution of polystyrene spheres, using an ultrafast optical Kerr gate (OKG). The results show that the time-resolved imaging of the target in the turbid media with an optical depth of 11.4 is achieved using the OKG with a 1.6 ps opening time. The image contrast is improved by about 70% compared with the shadowgraph imaging.

PACS: 42.65.-k, 42.62.-b

DOI:10.1088/0256-307X/29/2/024207

Imaging of targets embedded in turbid media are important in industrial, military and biomedical applications. However, it is difficult to observe those targets because of the strong multiple scattering. To overcome this problem, many optical gating techniques have been proposed for optical imaging in turbid media, which include the spatial filtering technique, the coherence-gating technique,^[1] the time-gating technique^[2–4] and so on. Compared with spatial filtering, the time-gating technique has the ability to separate the forward scattered diffusive photons traveling collinearly with small diverging angles from ballistic photons with a higher spatial resolution. Compared with the coherence-gating technique, the time-gating technique can use ballistic and near-ballistic light to acquire sufficient signal levels for imaging an object that is hidden in a highly turbid medium.

Imaging of a target in turbid media using the optical Kerr gate (OKG), which is a time gate with mild spatial filtering, could enhance image quality.^[4–7] Recently, the OKG technique has been adapted for investigating the dynamics of spray breakup and vaporization in the near field of the liquid-fueled combustion of a high-speed rocket spray. The optical depth of the near field is high, while other approaches have failed to reveal the internal structure of this area.^[8–14] The experimental data from the interior of the injector are important for designing rocket nozzle geometries.

In this Letter, we demonstrate the ultrafast imaging of a target in turbid media using an OKG in the femtosecond time scale, in which the target is hidden either behind glass diffusers or in a solution of polystyrene spheres. The results show that the time-resolved imaging in the turbid media with the optical depth about 11.4 is achieved using the OKG for a 1.6 ps opening time.

When the photons in a laser pulse travel through turbid media, only a few photons keep their coherence and pass through in a straight line without being scattered. These photons are image-bearing ballistic photons and they will exit the turbid media first, because they take the shortest path length. The most randomly scattered photons are called diffusive photons. Slightly scattered photons are referred to as snake photons, which are slightly deviated from the ballistic direction. These photons can be used in imaging when there are insufficient ballistic photons, though with a lower spatial resolution. By selecting the ballistic photons and rejecting the diffusive photons using spatial filtering, time-gated imaging or coherence-based techniques, it is possible to obtain diffraction-limited image resolution. Here the OKG is a time gate, which consists of a pair of calcite-crossed polarizers with a Kerr medium between them. Meanwhile, the spatial dimension of the pump laser pulse radial profile automatically induces a spatial aperture at the Kerr medium. When the ultrafast OKG is opened, only the ballistic and snake photons arriving earlier can pass through the gate. Figure 1 shows schematically the laser pulse passing through turbid media and eliminating the diffusive light from the image-bearing light using OKG.

Imaging through turbid media was performed using an OKG with setup shown in Fig. 2. A Ti:sapphire laser system (FEMTOPOWER compact Pro), emitting 30 fs, 800 nm laser pulses at a repetition rate of 1 kHz, was used in our experiments. The laser beam was split into an imaging beam and a gating beam by using a beam splitter. A delay line was used to control the time delay between the gating pulse and the imaging pulse. The gating beam was focused into the Kerr medium by lens L_1 , and the polarization of the beam was rotated 45° by a $\lambda/2$ wave plate.

*Supported by National Basic Research Program of China under Grant No 2012CB921804, and the National Natural Science Foundation of China under Grant Nos 91123028 and 11074197.

**Corresponding author. Email: jinhaisi@mail.xjtu.edu.cn

© 2012 Chinese Physical Society and IOP Publishing Ltd

The linearly polarized imaging beam was introduced into the turbid media. The optical depth is up to 12 (transmission factor of $\sim 10^{-10}$). The disturbed imaging beam emerging from the turbid media was focused into the Kerr medium together with the gating beam. The gating beam overlapped the imaging beam in the Kerr medium to ensure that the ballistic component could pass through the OKG. In addition, very few diffusive photons could be overlapped by the gating beam and pass through the OKG for the limited gating beam radius. The viewing area of the images will increase with the increasing overlapped area between the imaging beam and the gating beam. The OKG consists of a pair of calcite crossed polarizers and a Kerr medium between them. When the gating pulse causes a transient birefringence in the Kerr medium, the imaging beam will pass through the analyzer and be detected by a color charged-coupled device (CCD) camera (NIKON DXM 1200 F).

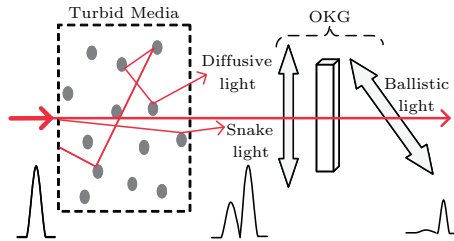


Fig. 1. Schematic diagram of a laser pulse passing through turbid media and eliminating the diffusive light from the image-bearing light using the OKG method.

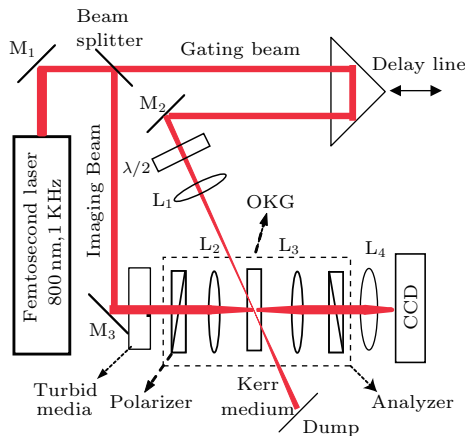


Fig. 2. Schematic setup for imaging in turbid media using the OKG method, L: lenses; M: mirrors; $\lambda/2$: half wave plate.

In our experiments, the Kerr medium CS_2 solution was filled in a glass cuvette with a path length of 1 mm. The opening time of the OKG for CS_2 is estimated to be 1.6 ps. The result is in agreement with the previous reports and indicates the reliability of our experiment.^[15–17] The measured temporal Kerr intensity profile of the transmitted signal through the solution of polystyrene spheres ($0.4 \mu\text{m}$) with the optical depth of 12 is shown in Fig. 3 (hollow circle). We

also plot a reference Kerr signal from the deionized water reference sample (solid square). The ballistic peak corresponds to the incident pulse, and there is no obvious diffusive peak separating from the ballistic peak. The reason is that the diameter of the polystyrene spheres used in our experiment is so small that the forward scattering probability is very low for these particles.^[18] Therefore, only a few diffusive photons can scatter in the forward direction and pass through the OKG.

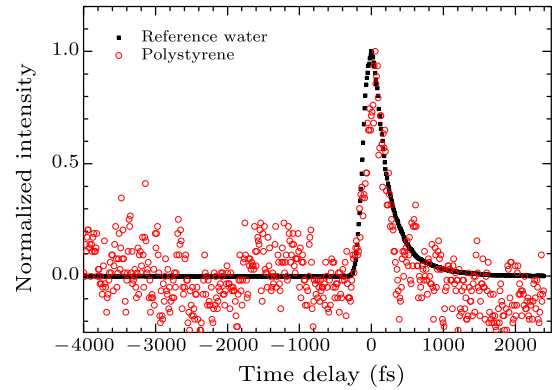


Fig. 3. The measured temporal Kerr intensity profile of the transmitted signal through the solution of polystyrene spheres with the optical depth of 12 (hollow circle). We also plot a reference Kerr signal from the deionized water reference sample (solid square).

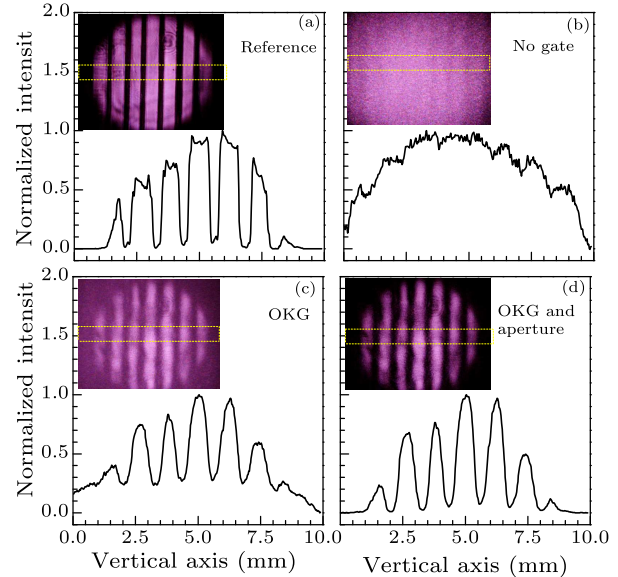


Fig. 4. Comparison of diffusive and OKG imaging of a bar chart hidden behind glass diffusers and the corresponding normalized intensity distributions in the rectangle as a function of CCD spatial position. (a) Reference imaging without the glass diffusers (ground glass). (b) Direct shadowgraph imaging. (c) OKG imaging. (d) OKG imaging with an aperture before the CCD.

The target sample is dark bars on a transparency sheet, the width of each bar is about 0.5 mm, and the direct shadowgraph imaging is shown in Fig. 4(a). Figure 4(b) represents the transillumination imaging

of the target bar chart hidden behind the glass diffusers with the optical depth of 7.26, and the image of

the bar chart is blurred. The measurement methods of the optical depth can be consulted in Ref. [19].

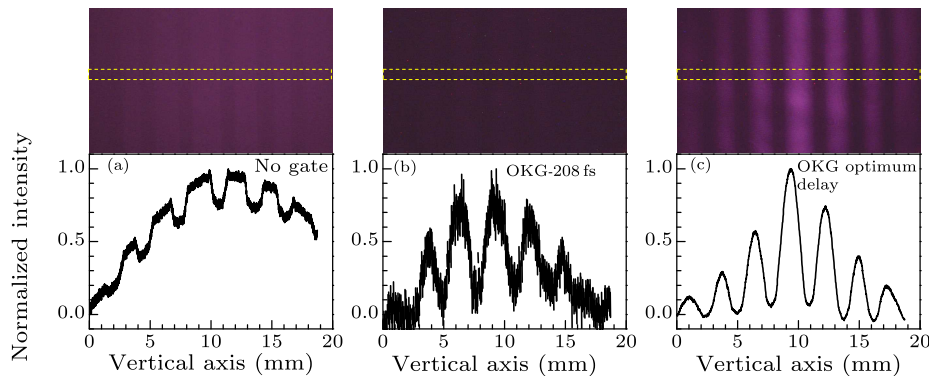


Fig. 5. Time-resolved OKG imaging of the target bar chart hidden in the polystyrene spheres of diameter $0.4\text{ }\mu\text{m}$ suspension and the corresponding normalized intensity distributions in the rectangle as a function of CCD spatial position. (a) Direct shadowgraph imaging. (b) Gating time at -208 fs . (c) Gating time at optimum delay.

To estimate the imaging quality, we calculate the contrast values from the intensity contribution. The contrast of the intensity field is calculated as $(I_{\text{max}} - I_{\text{min}}) / (I_{\text{max}} + I_{\text{min}})$, where I_{max} and I_{min} are the maximum and minimum image intensities, respectively. Assuming that the value of the contrast of the image in Fig. 4(a) is 1, and the value in Fig. 4(b) by direct shadowgraph imaging decreases to about 3%. Figure 4(c) presents the image using the OKG imaging technique, in which most of the diffusive photons are separated from the ballistic photons. The image contrast is increased to about 38% compared to the shadowgraph imaging, but there are some noises coming from the scattering pump pulse. Because the output laser beam has a Gaussian intensity profile, the normalized intensity of the image is stronger in the center than at the edges. The gating beam background signal noise also has a Gaussian intensity profile, as shown in Fig. 4(c), which causes the contrasts of the image to be non-unique for the center and the edges. To reduce these noises, in the experiment an aperture was added before the CCD and the estimated contrast increased to about 76% in comparison to the shadowgraph image shown in Fig. 4(d).

As an alternative turbid medium, a water solution of polystyrene spheres with diameter of $0.4\text{ }\mu\text{m}$ was used. The solution was filled in a quartz cell with thickness of 10 mm and the target bar chart was embedded in the middle of the cell and the optical depth measured to be about 11.4. Figure 5(a) shows the direct shadowgraph imaging of the target bars hidden in the polystyrene sphere suspension and the image was blurred. Figures 5(b) and 5(c) show the images of the target bar using the OKG at the non-optimum delay and the optimum delay between the image and the pump pulse. When the gating pulse arrived 208 fs

earlier than the optimum delay, the bar chart is hard to see and the image contrast is poor, as shown in Fig. 5(b). Figure 5(c) shows the clear bar chart image at the optimum delay between the imaging and the gating pulse and the contrast is improved from about 16% to 87%. The results suggest the feasibility of the imaging of targets hidden in turbid media using the OKG technique with submillimeter spatial resolution.

In summary, we have demonstrated the ultrafast imaging of a target in turbid media using an OKG for a 1.6 ps opening time. The results show that the time-resolved imaging of the submillimeter bar chart in the turbid media with optical depth of about 11.4 are achieved using the OKG and the image contrasts using the OKG are improved by about 70% in comparison with using direct shadowgraph imaging.

References

- [1] Huang D et al 1991 *Science* **254** 1178
- [2] Yoo K M and Alfano R R 1990 *Opt. Lett.* **15** 320
- [3] Fujimoto J G et al 1986 *Opt. Lett.* **11** 150
- [4] Wang L et al 1991 *Science* **253** 769
- [5] Alfano R R et al 1994 *Science* **264** 1913
- [6] Wang L et al 1993 *Opt. Lett.* **18** 241
- [7] Wang L, Ho P P and Alfano R R 1993 *Appl. Opt.* **32** 535
- [8] Paciaroni M and Linne M 2004 *Appl. Opt.* **43** 5100
- [9] Paciaroni M et al 2006 *Atomization and Sprays* **16** 51
- [10] Gord J et al 2005 *Appl. Opt.* **44** 6627
- [11] Hall T et al 2006 *Exp. Fluids* **40** 836
- [12] Sedarsky D L et al 2006 *Opt. Lett.* **31** 906
- [13] Schmidt J B et al 2008 *Appl. Opt.* **48** B137
- [14] Idlahcen S, Blaisot J B, Girasole T Rozé and Mées L 2008 *14th International Symposium on Applications of Laser Techniques to Fluid Mechanics* (Lisbon, Portugal, 7–10 July 2008)
- [15] Yan L et al 2009 *IEEE Photon. Technol. Lett.* **21** 1606
- [16] Tan W et al 2010 *J. Appl. Phys.* **107** 043104
- [17] Kalpouzos C et al 1987 *J. Phys. Chem.* **91** 2028
- [18] Berrocal E et al 2007 *Opt. Express* **15** 10649
- [19] Tong J et al 2011 *Opt. Eng.* **50** 043607